

Molecular Structures of Chloro(phthalocyaninato)-aluminum(III) and -gallium(III) as Determined by Gas Electron Diffraction and Quantum Chemical Calculations: Quantum Chemical Calculations on Fluoro(phthalocyaninato)-aluminum(III) and -gallium(III), Chloro(tetrakis(1,2,5-thiadiazole)porphyrizinato)-aluminum(III) and -gallium(III) and Comparison with their X-ray Structures

Tatyana Strenalyuk, Svein Samdal,* and Hans Vidar Volden

Centre for Theoretical and Computational Chemistry (CTCC), Department of Chemistry, University of Oslo, P.O. Box 1033 Blindern, NO-0315 Oslo, Norway

Received: May 9, 2008; Revised Manuscript Received: July 7, 2008

The molecular structures of chloro(phthalocyaninato)aluminum(III) (ClPcAl) and chloro(phthalocyaninato)-gallium(III) (ClPcGa) have been determined by using the gas electron diffraction (GED) method and augmented by quantum chemical calculations. The molecular structures of fluoro(phthalocyaninato)aluminum(III) (FPcAl), fluoro(phthalocyaninato) gallium(III) (FPcGa), chloro(tetrakis(1,2,5-thiadiazole)porphyrizinato)aluminum(III) (ClTTDPzAl), and chloro(tetrakis(1,2,5-thiadiazole)porphyrizinato)gallium(III) (ClTTDPzGa) have been optimized at the level B3LYP with basis sets 6-31G*, 6-311++G**, and cc-pVTZ, and the structures have been compared with those obtained by X-ray diffraction. Vibrational frequencies have been calculated for all six molecules at all basis sets combinations, except B3LYP/cc-pVTZ. These calculations predict that all molecules have C_{4v} symmetry with the metal atom above the plane defined by the four inner cavity N atoms and an almost planar macrocycle. The most important structure parameters (GED|B3LYP/cc-pVTZ) are h (height of the metal atom above the inner cavity) $h = 50.3(32)|44.9$ pm, $r(\text{Al}-\text{Cl}) = 214.5(16)|217.4$ pm, $r(\text{Al}-\text{N}) = 197.6(9)|198.7$ pm, $\angle(\text{Cl}-\text{Al}-\text{N}) = 104.8(9)|103.1^\circ$, $\angle(\text{Al}-\text{N}-\text{C}) = 124.2(7)|125.9^\circ$ for ClPcAl, and the corresponding values for ClPcGa are $h = 53.1(28)|50.2$ pm, $r(\text{Ga}-\text{Cl}) = 218.9(14)|222.3$ pm, $r(\text{Ga}-\text{N}) = 200.6(8)|202.6$ pm, $\angle(\text{Cl}-\text{Ga}-\text{N}) = 105.4(8)|104.3^\circ$, $\angle(\text{Ga}-\text{N}-\text{C}) = 123.8(8)|125.0^\circ$. Parenthesized values are estimated error limits defined as $2.5(\sigma_{\text{lsq}}^2 + (0.001 \times r)^2)^{1/2}$ for distances and $2.5\sigma_{\text{lsq}}$ for angles. The title compounds are all flexible molecules with about five vibrational frequencies below 100 cm^{-1} .

Introduction

Metal phthalocyanines (MPcs) represent a class of molecules which attracts great attention in many different fields of science and industry. Their high thermal and chemical stability have made them suitable for many technological applications as dyes, pigments, semiconductors, energy conversion in photovoltaic and solar cells, photosensitizers, electrophotography, molecular electronics, gas sensors, electrochromism in display devices, liquid crystals, Langmuir–Blodgett films, nonlinear optics, electrocatalytic reagents, and photodynamic therapy. Because of the similarity in structure to biologically important molecules such as chlorophyll and hemoglobin, they have attracted special interest. There are several excellent books about phthalocyanines where the above-mentioned properties and applications are discussed.^{1–6}

We have recently determined the molecular structure of a F-substituted subphthalocyanine (SubPc(F)),⁷ phthalocyaninatozinc compounds (Pc(H)Zn and Pc(F)Zn)⁸ and metal-free phthalocyanine (H₂Pc)⁹ by using gas electron diffraction (GED) and high-level quantum chemical calculations. These investigations have shown that GED is able to obtain accurate molecular structures compared to previous gas-phase investigations^{10,11} and that B3LYP calculations are consistent with the experimentally determined structures. These results have motivated us to further work on metallophthalocyanines, specifically on Group 13 and

Group 14 compounds which hold considerable interest because of their chemical stability and the high conductivity of their partially oxidized derivatives. The experimental work reported here concerns the molecules chloro(phthalocyaninato)aluminum (ClPcAl) and chloro(phthalocyaninato)gallium (ClPcGa) which are similar to the molecules just mentioned. As far as we know, the gas-phase structures of ClPcAl and ClPcGa are unknown, but the crystal structures of ClPcGa and its homologue FPcGa have been measured. It is curious that these are rather different; details are found in the Results and Discussion section.

We have also carried out molecular orbital calculations on both ClPcAl and ClPcGa and four similar compounds fluoro(phthalocyaninato)aluminum(III) (FPcAl), fluoro(phthalocyaninato)gallium(III) (FPcGa), chloro(tetrakis(1,2,5-thiadiazole)porphyrizinato)aluminum(III) (ClTTDPzAl), and chloro(tetrakis(1,2,5-thiadiazole)porphyrizinato)gallium(III) (ClTTDPzGa). It was hoped that these calculations would give information about structural changes of the cavity of the Pc upon changes in the axial and peripheral environment.

Systematic names for the two molecule studies by GED are chloro[29H,31H-phthalocyanato(2-)-κN29,κN30,κN31,κN32]-aluminum (ClPcAl) and chloro[29H,31H-phthalocyanato(2-)-κN29,κN30,κN31,κN32]gallium (ClPcGa).

Experimental and Computational Section

GED. A brief description of the electron diffraction method is given in a recent article on a similar molecule SubPc(F).⁷

* Corresponding author. E-mail: svein.samdal@kjemi.uio.no. Phone: 47 2285 5458. fax +47 2285 5441.

TABLE 1: Experimental Conditions for CIPcM (M = Al, Ga)

	CIPcAl		CIPcGa	
nozzle-to-plate distance/mm	498.67	248.71	498.52	248.83
electron wavelength/pm	5.82	5.82	5.82	5.82
nozzle temperature/°C	468	468	428	428
<i>s</i> range/nm ⁻¹ , <i>x</i> -direction	17.50–152.50	35.00–302.50	17.50–152.50	35.00–302.50
<i>s</i> range/nm ⁻¹ , <i>y</i> -direction	17.50–133.75	35.00–245.00	17.50–122.50	40.00–245.00
$\Delta s/\text{nm}^{-1}$	1.25	1.25	1.25	1.25
number of plates	4	4	4	4
degree of polynomial ^a	8	10	8	10

^a Degree of polynomial used in the background subtraction.

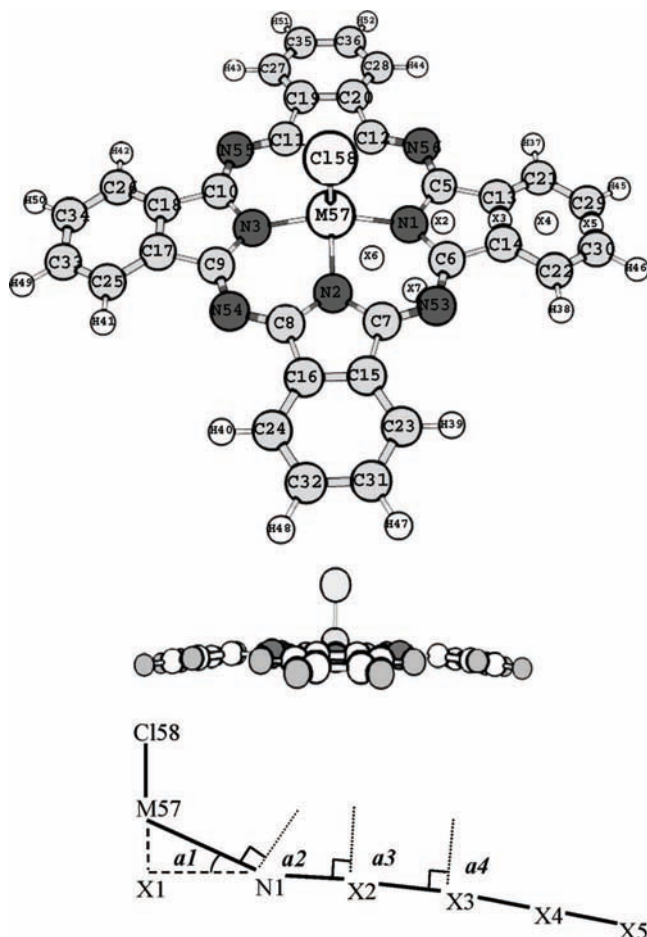


Figure 1. Numbering of the atoms for CIPcM (M = Al, Ga) and some auxiliary points X1–X5.

This article may help evaluating the experimental data, the strategies chosen for least-squares refinement, and the precision and accuracy of the structure parameters.

CIPcAl and CIPcGa were obtained from Aldrich and used without further purification.

The GED data were recorded on the Balzers KD-G2 unit at the University of Oslo, and the experimental setup is the same as for Pc(H)Zn and Pc(F)Zn.⁸ The experimental conditions are summarized in Table 1.

Quantum Chemical Calculations. The quantum chemical calculations were performed by using the GAUSSIAN03 program package¹⁵ running on the HP superdome-facilities in Oslo.

B3LYP^{16,17} has been widely used for Pcs and similar systems. Our previous quantum chemical calculations on SubPc(F), Pc(H)Zn, Pc(F)Zn, and H₂Pc with different methods and basis sets confirm that B3LYP gives good agreement with the

experimental results,^{7,8} and it is expected that the B3LYP calculations would give similar good results for the title compounds.

The basis sets we have used are 6-31G*, 6-311++G**,^{18,19} and cc-pVTZ.²⁰ To our knowledge, the present calculations represent the highest level performed so far on these molecules. The numbering of the atoms is shown in Figure 1. The most important calculated structure parameters are given in Tables 2 and 3.

Molecular force field calculations were made in order to ensure that the stationary points represent true minima, except for the cc-pVTZ basis set which is too time-consuming.

The reliability of the IR and Raman intensities are improved by introduction of diffuse and polarization functions.^{21–24} Calculated frequencies and IR intensities obtained by using B3LYP/6-311++G** are given as Supporting Information for all title compounds as well as their Cartesian coordinates from the B3LYP/cc-pVTZ calculations.

Structure Refinement on CIPcM (M = Al, Ga). According to the quantum chemical force field calculations, all the title molecules have *C*_{4v} symmetry with a square-pyramidal coordination of the metal atom with the halogen atom in the apical and the four isoindole N atoms in the basal positions. The numbering of the atoms in CIPcM and CITTDPzM is shown in Figures 1 and 2, respectively.

Because of the structural similarity of CIPcAl and CIPcGa, they may be described by one model where the Pc ligand is obtained by rotations of one isoindole unit (N1, C5, C6, C13, C14, C21, C22, C29, C30, H37, H38, H45, H46) around the 4-fold symmetry axis. Bending angles of the ring system were used to model the concave shape of the Pc macrocycle.

The following independent parameters were chosen to describe the molecular geometry. These parameters are (bond distances) M57–C158, N1–M57, N1–C5, C5–C13, C13–C14, C21–H37, M57–C158 and (bond angles) C5–N1–C6, C14–C13–C21, C13–C21–H37, C21–C29–H45. The dihedral angles C14–C13–C21–H37 and C13–C21–C29–H45 were fixed at 180° in agreement with the quantum chemical calculations. The shape of the Pc ligand is defined by four angles, *a*1–*a*4, see Figure 1. The following angles define bending of the Pc: M57–N1–X1 = *a*1, where X1 is at the center of the N₄ cavity formed by the four isoindole N atoms and *h* = M–X1 is equal to the height of atom M above the N₄ plane. M57–N1–X2 = (*a*2 + 90°) defines the concave shape of the Pc macrocycle, N2–X2–X3 = (*a*3 + 90°) angle defines the nonplanarity of the pyrrole ring and is equal to the envelope angle (dihedral angle N1–C5–C6–C14) of the pyrrole ring, and X2–X3–X4 = (*a*4 + 90°) corresponds to folding of the isoindole unit about C13–C14 bond. The positions of the bridged N atoms (N53 to N56) are determined by the N53–X7–X6 angle and the dihedral angle M57–X6–X7–N53 which gives a boat conformation (0°) or a chair

TABLE 2: Selected Structure Parameters^a Obtained by B3LYP Calculations by Using basis sets 6-311++G(A) and cc-pVTZ(B) and X-ray Diffraction**

	ClPcAl			ClPcGa			FPcAl	FPcGa	
	A	B	X-ray ^{13b}	A	B	X-ray ¹³	B	B	X-ray ^{14c}
Bond Lengths, pm									
X58–M57	217.4	217.8	218	222.3	222.0	221.1	169.3	179.2	193.0
N1–M57	198.7	198.4	198	202.6	202.6	198.3	198.5	202.1	197.0
N1–C5	138.0	137.7	144	137.7	137.3	138.1	137.6	137.3	137.5
C5–C13	145.2	144.9	137	145.5	145.2	144.8	145.0	145.2	145.3
C5–N56	131.9	131.6	136	132.2	131.9	132.0	131.7	131.9	133.0
C13–C14	140.2	139.9	136	140.5	140.1	138.1	139.9	140.2	139.0
C13–C21	139.5	139.2	146	139.5	139.1	138.6	139.1	139.1	138.9
C21–C29	139.0	138.7	141	139.1	138.7	137.6	138.7	138.7	138.4
C29–C30	140.8	140.4	141	140.7	140.3	138.4	140.4	140.3	138.4
C21–H37	108.3	108.1		108.3	108.1	88.7	108.1	108.1	87.4
C29–H45	108.4	108.2		108.4	108.2	99.0	108.2	108.2	83.1
N1...N3	387.0	386.2	387	392.6	392.2	386.7	386.5	392.6	393.8
N1...N2	273.7	273.1	273	277.6	277.3	273.4	273.3	277.6	278.4
Bond Angles, degree									
N1–M57–X58	103.1	103.3	103	104.3	104.5	102.8	103.2	103.7	90.0
C5–N1–M57	125.7	125.6	122	125.0	125.0	125.9	125.6	125.0	125.5
C5–N1–C6	107.5	107.5	103	108.6	108.7	107.0	107.5	108.7	108.6
N1–C5–C13	109.8	109.8	109	109.1	109.1	109.3	109.8	109.0	108.9
C5–C13–C14	106.5	106.5	109	106.6	106.6	107.0	106.5	106.6	106.8
C5–N56–C12	122.6	122.7	126	123.5	123.7	122.6	122.8	123.7	123.0
C14–C13–C21	121.2	121.2	122	121.2	121.2	121.1	121.2	121.2	121.1
C13–C21–C29	117.5	117.6	116	117.6	117.6	117.6	117.6	117.7	117.3
C21–C29–C30	121.2	121.2	122	121.2	121.2	121.3	121.2	121.2	121.4
C13–C21–H37	120.8	120.8		120.8	120.8	118.6	120.8	120.8	121.5
C21–C29–H45	119.6	119.7		119.6	119.6	127.4	119.6	119.6	120.8
Dihedral Angles, degree									
M57–N1–C5–C13	167.4	167.1	165	166.6	166.5	166.4	167.1	167.3	172.4
C5–C13–C14–C22	179.7	179.7	175	179.5	179.5	179.0	179.7	179.6	178.6
N1–C5–C6–C14	179.4	179.4	174	179.4	179.4	179.1	179.4	179.4	179.5
N53–C7–C6–N1	178.8	178.8	176	178.6	178.5	179.3	178.1	178.7	178.7
C14C13C21H37	180.0	178.0		179.9	179.9	175.8	180.0	179.9	178.6
C13C21C29H45	–179.8	–179.8		–179.7	–179.7	177.2	–179.8	–179.8	179.3

^a Numbering of the atoms is shown in Figure 1. The parameters given for the solid state represent average values. ^b Crystal structure is disordered. ^c FPcGa is polymeric in the solid phase: [PcGa- μ F]_∞.

conformation (180°) of the six-membered (M57, N1, C6, N53, C7, N2) ring. X1–X7 are all auxiliary points, see Figure 1.

It is difficult to determine accurately the difference between bond lengths of similar magnitude. Therefore, some constraints had to be used in the structural analysis and these are C13–C21 = C13–C14 + Δ 1, C21–C29 = C13–C14 + Δ 2, C29–C30 = C13–C14 + Δ 3, C29–H45 = C21–H37 + Δ 4, and N53–C6 = N1–C5 + Δ 5. The differences, Δ 1–5, were taken from the B3LYP/6-311++G** calculations, and they are –0.72, –1.19, 0.56, 0.12, and –6.10 pm for ClPcAl and –1.01, –1.37, 0.24, 0.11, and –5.49 pm for ClPcGa, respectively. Because of the low scattering power of the H atoms, it was not possible to determine the bond angles involving H atoms with reasonable accuracy, and therefore, these angles were fixed at their calculated values.

Vibrational Corrections. The root-mean-square amplitudes of vibration, u values, and shrinkage correction coefficients, k values, used in the GED analysis were calculated from the B3LYP/6-311++G** force fields by using the SHRINK program.^{25,26} The SHRINK program calculates the shrinkage corrections by using two different approaches. One approach is based on a rectilinear^{27,28} movement of the atoms, and the other is based on a curvilinear^{25,26} movement of the atoms. The latter approach is generally considered to be the more realistic, and this approach (k_{h1} values) has been used in this investigation. The amplitudes of distances within one peak in the RD-curves (Figures 3 and 4) were refined with constant differences. The

KCED25²⁹ least-squares fitting program was used to obtain structure parameters.

The $r_e - r_a$ correction terms, that is, the differences between the bond distances obtained by GED (r_a) and quantum chemical calculations (r_e), were estimated by the SHRINK program and are used to obtain the final results listed in Tables 5 and 6.

Results and Discussion

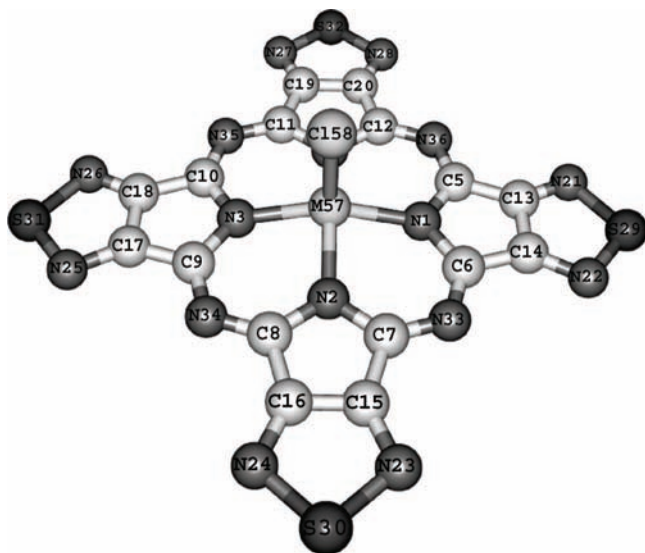
Quantum Chemical Calculations and Comparison with X-ray Structures. The most important structure parameters for ClPcAl, ClPcGa, FPcAl, and FPcGa together with available crystallographic parameters are given in Table 2, and similar data for ClTDPzAl and ClTDPzGa are given in Table 3. Cartesian coordinates for the optimized molecular structures for all six molecules obtained from B3LYP/cc-pVTZ calculations are given as Supporting Information (Tables S3–S8).

The structural parameters related to the isoindole unit do not change much for the four Pcs as can be seen from Table 2. It should be noted that the structural parameters for the isoindole unit in ClPcAl and FPcAl are almost identical. This is also the case when the structural parameters for the isoindole units in ClPcGa and FPcGa are compared. These results strongly indicate that the halogen atom in apical position have negligible influence on the structure of the isoindole unit. Furthermore, it should also be noted that the structural differences between the isoindole units in ClPcAl and ClPcGa are small but significant. Almost

TABLE 3: Selected Structure Parameters^a Obtained by B3LYP/cc-pVTZ Calculations and X-ray Diffraction

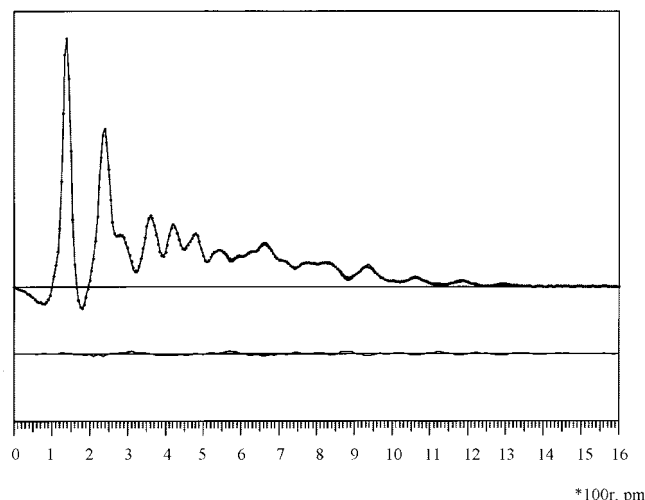
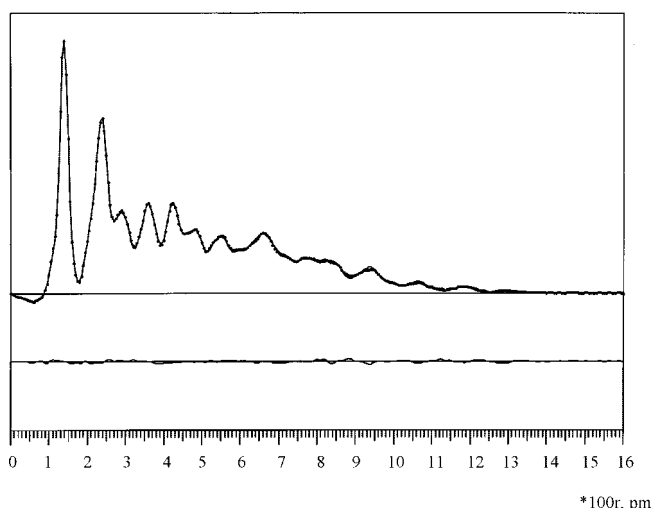
	CITDPzAl	X-ray ³⁰	CITDPzGa	X-ray ³⁰
Bond Lengths, pm				
X58–M57	216.2	217.0	220.5	219.4
N1–M57	200.8	200.0	204.9	201.2
N1–C5	138.4	139.6	138.0	138.6
C5–C13	145.0	145.5	145.3	145.3
C5–N56	131.0	132.9	131.2	132.0
C13–C14	141.2	141.3	141.6	139.6
C13–N21	131.2	132.5	131.7	133.0
N21–S29	165.1	162.6	165.2	163.8
N1···N3	391.5	391.2	395.6	392.5
N1···N2	276.9	276.6	281.1	277.5
Bond Angles, degree				
N1–M57–X58	102.9	102.0	104.0	102.7
C5–N1–M57	124.8	125.1	124.1	124.7
C5–N1–C6	109.2	108.6	110.5	109.2
N1–C5–C13	108.5	108.6	107.7	108.1
C5–C13–C14	106.9	107.1	107.1	107.3
C5–N56–C12	123.3	121.3	124.2	122.4
C14–C13–N21	115.2	114.4	115.2	115.2
C13–N21–S29	104.6	105.4	104.7	104.2
N21–S29–N22	100.4	100.5	100.3	101.2
Bond Angles, degree				
M57–N1–C5–C13	167.3	168.1	166.6	167.4
C5–C13–C14–N21	179.6	179.1	179.5	178.7
N1–C5–C6–C14	179.2	179.5	179.0	178.9
N53–C7–C6–N1	178.9	176.8	178.7	178.6

^a Numbering of the atoms is shown in Figure 2. The parameters given for the solid state represent average values.

**Figure 2.** Numbering of the atoms for CITDPzM (M = Al, Ga).

identical structure differences within the isoindole unit are obtained when the corresponding structure parameters in FPcAl and FPcGa are compared. This indicates that the metal atom causes a small but significant structural change on the isoindole unit.

It is also interesting to compare the structural differences in the pyrrole ring for corresponding structural parameters in CITDPzAl and CITDPzGa and compare those with the differences in the pyrrole ring found in CIPcAl and CIPcGa, and FPcAl and FPcGa. The structural differences within the isoindole unit are almost identical, which indicates that the peripheral ring system has negligible influence on the structural differences in the pyrrole ring and that those differences are

**Figure 3.** Radial-distribution (RD) curves for CIPcAl. The experimental points (dots) are the average of the four curves shown in Figure 5, and theoretical points were used for the unobserved region $s < 17.50 \text{ nm}^{-1}$. The damping coefficient for the RD function is 35 pm^2 . The difference curve is experimental curve minus theoretical curve.**Figure 4.** RD curves for CIPcGa. The experimental points (dots) are the average of the four curves shown in Figure 6, and theoretical points were used for the unobserved region $s < 17.50 \text{ nm}^{-1}$. The damping coefficient for the RD function is 35 pm^2 . The difference curve is experimental curve minus theoretical curve.**TABLE 4: Barrier to Planarity and M–X Stretching Frequencies for the Six Title Compounds**

compound	barrier (kJ/mol)	M–X(calc, cm^{-1})	M–X(obs, cm^{-1})
FPcAl	103.1	745	550 ³¹
FPcGa	74.7	597	517 ³¹
CIPcAl	88.8	489	440 ³⁰
CIPcGa	89.3	362	351 ³⁰
CITDPzAl	84.6	501	345 ³⁰
CITDPzGa	84.1	376	382 ³⁰

due to replacement of the Al atom with a Ga atom. However, the absolute values of the structure parameters for the pyrrole ring cause a small but significant change when a benzene ring is replaced with a 1,2,5-thiadiazole ring.

Replacing the smaller Al atom with the larger Ga atom in Pc complexes increases the diameter of the inner cavity by about 6 pm. The same increase is also found for the TDPz complexes as seen in Table 3.

Comparing the structural parameters for CIPcAl obtained from B3LYP/cc-pVTZ calculations with those obtained by X-ray¹³

TABLE 5: Selected Structure Parameters for ClPcAl^a

parameter	GED		B3LYP 6-311++G**		B3LYP cc-pVTZ	X-ray ¹³
	r_e	u_{exp}	u_{h1}^b	k_{h1}^b	r_e	
Bond Lengths, pm						
$h(\text{Al})^c$	50.3(32)				44.9	41
Al57–Cl58	214.5(16)	8.6(3)	7.6	–3.196	217.4	218
Al57–N1	197.6(9)	9.0(3)	8.1	–0.674	198.7	198
N1–C5	139.5(7)	5.6(3)	5.2	–1.172	138.0	144
C5–C13	145.8(8)	5.7(3)	5.3	–1.452	145.2	137
C13–C14	139.3(5)	5.3(3)	4.9	–1.853	140.2	136
C13–C21 ^d	138.7(5)	5.3(3)	4.9	–2.740	139.5	146
C21–C29 ^d	138.3(5)	5.2(3)	4.9	–2.798	139.0	141
C29–C30 ^d	140.0(5)	5.4(3)	5.0	–2.770	140.8	141
C21–H37	111.1(12)	7.9(3)	7.6	–3.563	108.3	
C29–H45 ^d	111.2(12)	7.9(3)	7.6	–3.947	108.4	
C6–N53 ^d	132.6(7)	5.0(3)	4.7	–1.176	131.9	136
Bond Angles, degree						
Cl58–Al57–N1 ^e	104.8(9)				103.1	103
Al57–N1–C5 ^e	124.2(7)				125.7	122
C5–N1–C6	105.8(9)				107.5	103
C14–C13–C21	121.1(4)				121.2	122
C13–C21–C29 ^e	117.7(7)				117.5	
C13–C21–H37 ^f	120.8				120.8	
C21–C29–H45 ^f	119.6				119.6	
C6–N53–C7 ^e	121.1(7)				122.6	126
N1–C6–N53 ^e	127.5(5)				127.5	123
Bending Angles, degree						
a_1	14.8(9)				13.1	13
a_2	68.7(35)				81.2	
a_3	95.8(61)				90.6	
a_4	97.9(44)				90.3	
N53–X7–X6	89.8(87)				88.8	
Al57–X6–X7–N53	0.0				0.0	
$R_f\%$	4.80 ^g					

^a Parenthesized values are estimated error limits defined as $2.5(\sigma_{\text{lsq}}^2 + (0.001 \times r)^2)^{1/2}$ for distances and $2.5\sigma_{\text{lsq}}$ for angles and amplitudes, where σ_{lsq} is one standard deviation taken from the least-squares refinements by using a diagonal weight matrix and the $0.001 \times r$ term represent 0.1% uncertainty in the electron wavelength. The errors are in the units of the last digits. ^b Curvilinear treatment of the vibrating atoms (by SHRINK program). ^c r_a parameter. $h(\text{Al})$ is the height of the Al atom above the inner cavity plane of the N atoms. ^d This value was calculated by using constraints between parameters (see text). ^e Dependent parameter. ^f This parameter was fixed at its B3LYP/6-311++G** calculated values. ^g Goodness-of-fit parameter.

(Table 2) reveals substantial differences. These differences must be related to the fact that the crystal structure is disordered; therefore, a closer comparison is not justified.

Two X-ray investigations exist for ClPcGa, a single-crystal X-ray analysis¹³ (R factor = 0.042) and a powder crystal Rietveld analysis¹² (R factor = 0.216). The Ga–Cl bond length is completely different for these two investigations where the Rietveld analysis obtains a Ga–Cl bond length of 202.1 pm to be compared with 221.1 pm in the single-crystal X-ray analysis and 222.0 pm from the B3LYP/cc-pVTZ calculation. Only structure parameters from the single-crystal X-ray analysis and the B3LYP calculation are given in Table 2, and as can be seen, there is a generally good agreement between these parameters.

The structure of the monomeric FPcGa is calculated to be similar to that of the Cl analogue. The coordination polyhedron of Ga is square pyramidal with the F atom in the apical position and the four isoindole N atoms in basal position. An investigation by X-ray crystallography showed that FPcGa is polymeric in the solid phase: $[\text{PcGa}-\mu\text{F}]_{\infty}$. The Ga atom is octahedral with the two F atoms in trans positions. The two Ga–F bonds are about 14 pm longer than calculated for the monomeric form, and the Ga–N bonds are about 5 pm shorter. An elongation of 3.7 pm for the Ga–F bond length and a 3.3 pm shortening of the Ga–N bond length is obtained from a B3LYP/6-31G* calculation when the Ga atom is forced to be in the center of the inner cavity and a planar Pc macrocycle. In Table 4, the

barriers toward planarity for all the six title compounds are given. It is only for FPcGa that the Ga atom is found to be located at the center of the inner cavity in the solid phase, and from the B3LYP/6-31G* calculation, this molecule also has the lowest barrier toward planarity. The size of the inner cavity increases by less than 1 pm as seen from Table 2. It should be noted that there is surprisingly good agreement between the structure parameters for the isoindole unit obtained from B3LYP/cc-pVTZ calculation and those determined by X-ray, as seen in Table 2.

In Table 3, the X-ray structures are compared with the B3LYP/cc-pVTZ optimized structures for ClTDPzAl and ClTDPzGa. The single crystals for those two compounds were grown by vacuum sublimation, but the level of their crystallinity was not very high.³⁰ The average of symmetry equivalent structure parameters according to C_{4v} symmetry for the solid-state parameters give a surprisingly good agreement with their calculated values, as seen in Table 3.

Molecular Vibrations and Flexibility. The MPcs have often been regarded as rigid molecules, but this is a rather doubtful description because five or more vibrational frequencies are usually found below 100 cm^{-1} according to the B3LYP/6-311++G** calculations. The five lowest vibrational frequencies are all out-of-plane motions. The lowest B_2 mode can best be described as two opposite isoindole units moving up and the other two down. The A_1 mode is a breathing motion where all

TABLE 6: Selected Structural Parameters ClPcGa^a

parameter	GED		B3LYP 6-311++G**		B3LYPcc-pVTZ	X-ray ¹³
	r_e	u_{exp}	u_{hl}^b	k_{hl}^b	r_e	
Bond lengths, pm						
$h(\text{Ga})^c$	53.1(28)				50.2	43.9
Ga57–Cl58	218.9(14)	8.3(5)	7.6	–3.813	222.3	221.8
Ga57–N1	200.6(8)	8.8(5)	8.1	–0.733	202.6	198.3
N1–C5	139.1(6)	5.3(3)	5.2	–1.082	137.7	138.1
C5–C13	146.3(8)	5.5(3)	5.3	–1.346	145.5	144.8
C13–C14	140.0(5)	5.0(3)	4.9	–1.554	140.5	138.1
C13–C21 ^d	139.0(5)	5.0(3)	4.8	–2.565	139.5	138.6
C21–C29 ^d	138.7(5)	5.0(3)	4.8	–2.609	139.1	137.6
C29–C30 ^d	140.2(5)	5.2(3)	5.0	–2.419	140.7	138.4
C21–H37	112.0(16)	7.7(3)	7.5	–3.241	108.3	88.7
C29–H45 ^d	112.1(16)	7.7(3)	7.6	–3.732	108.4	99.0
C6–N53 ^d	133.0(6)	4.8(3)	4.6	–1.021	132.2	132.0
Bending angles, degree						
Cl58–Ga57–N1 ^e	105.4(8)				104.3	102.8
Ga57–N1–C5 ^e	123.8(8)				125.0	125.9
C5–N1–C6	106.9(9)				108.6	107.0
C14–C13–C21	120.9(4)					121.2
C13–C21–C29 ^e	117.9(8)				117.6	117.6
C13–C21–H37 ^f	120.8				120.8	118.6
C21–C29–H45 ^f	119.6				119.6	127.4
C6–N53–C7 ^e	122.1(9)				123.5	122.6
N1–C6–N53 ^e	127.1(5)				127.6	127.4
Bending angles, degree						
a_1	15.4(8)				14.3	11.4
a_2	68.9(40)				79.6	
a_3	98.8(63)				90.6	
a_4	99.2(47)				90.5	
N53 × 7X6	81.2(48)				88.6	
Ga57 × 6X7N53	0.0				0.0	
$R_f\%$	6.54 ^g					

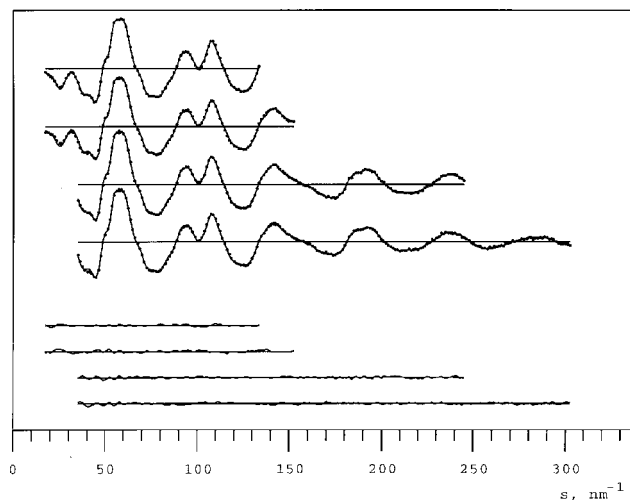
^a See footnotes to Table 5.

Figure 5. Average molecular intensity curves for the best model of ClPcAl. The first two curves are the average from eight sectors from the long camera distance along the y - and x -axis respectively. The two next curves are the corresponding average curves from eight sectors from the middle camera distance. Dots are experimental points, and full lines are the theoretical curves. The four curves below are difference curves. The difference curve is experimental curve minus theoretical curve.

isoindole units are moving either up or down. The B_1 mode is a twisting of the isoindole units as a propeller. The two next E modes can best be described as a butterfly-swimming motion and the other as an in-phase twisting out-of-plan of two opposite isoindole units whereas the two other isoindole units are only

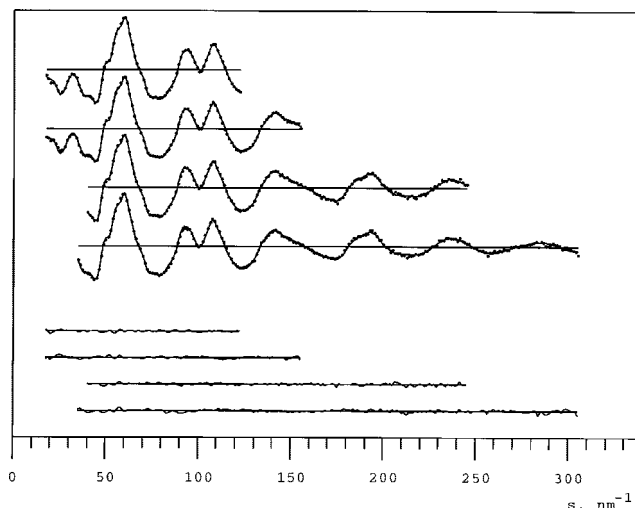


Figure 6. Average molecular intensity curves for the best model of ClPcGa. The first two curves are the average from eight sectors from the long camera distance along the y - and x -axis respectively. The two next curves are the corresponding average curves from eight sectors from the middle camera distance. Dots are experimental points, full lines are the theoretical curves. The four curves below are difference curves. The difference curve is experimental curve minus theoretical curve.

moving slightly. The lowest in-plane B_1 mode is twisting of the isoindole units. The motion of the metal atom together with the halogen atom which is moving in and out of the central cavity relative to the metal atom is in the region 150–170 cm^{-1} . Unfortunately, there is little information about the vibrational spectra for the title compounds. However, there is some

information about the M–X stretching frequencies, and those are given in Table 4. There are serious disagreements between the proposed assignment M–X stretching frequencies and their B3LYP/6-311++G** calculated frequencies. Only the Ga–Cl stretching frequency in ClPcGa and ClTTPzGa seems to be correctly assigned.

With many low vibrational modes, it is important to include the best available vibrational correction terms in the analysis of the GED data, and this was done by using the curvilinear approach and the SHRINK program as outlined in the Vibrational Corrections section.

Calculated vibrational frequencies and infrared intensities from B3LYP/6-311++G** are given as Supporting Information, Table S1 for ClPcAl, ClPcGa, FPcAl, and FPcGa and Table S2 for ClTTPzAl and ClTTPzGa.

Molecular Structures Determined by GED. The experimental GED structures are given in Tables 5 and 6 for ClPcAl and ClPcGa, respectively.

The bond lengths in ClPcAl are transformed to r_e parameters by using correction terms obtained from the SHRINK program, and these parameters are compared with their B3LYP/cc-pVTZ counterparts and X-ray values. There is a generally very good agreement between the GED structure and the B3LYP/cc-pVTZ structure, and the rather poor agreement with the X-ray structure is due to the translational disorder in the unit cell.¹³

Some of the bending angles (a_2 to a_4) have rather large error limits, and those parameters are not well determined by the GED method. This is certainly related to the flexibility of the macrocycle, and the question whether these GED-bending angles really are comparable with their theoretical counterparts should be raised. The r_a parameter from GED represents an average over all vibrational levels where each level is populated according to the Boltzmann distribution law. In this case, there are five different vibrational frequencies below 100 cm^{-1} , and all of them are related to out-of-plan motions. It is the structure parameters related to the planarity of the macrocycle which are mostly influenced by the low vibrational modes, and this is clearly shown in Table 5. Even if the curvilinear treatment of vibrating atoms is the best available approximation, it might be that it is not good enough for a proper description of the flexible isoindole subunits and thereby causing these disagreements.

The agreement between the observed and calculated u values is acceptable. The RD curves and intensity curves for the best model are shown in Figures 3 and 5, respectively.

The structure parameters for ClPcGa are handled in the same way as for ClPcAl and shown in Table 6, and the same statements can be made for ClPcGa as for ClPcAl. The single-crystal X-ray structure determined by Wynne¹³ is in excellent agreement with the calculated B3LYP/cc-pVTZ structure and with the GED structure. The RD curves and intensity curves for the best model are shown in Figures 4 and 6, respectively.

This study confirms that the GED method is able to derive accurate structure parameters for large macrocycles.

Concluding Remarks

All B3LYP calculations predict the molecular symmetry to be C_{4v} with the metal atom above the plane defined by the four inner cavity N atoms and an almost planar Pc macrocycle. This is supported by this GED investigation by showing excellent agreement to the experimental GED data as shown in Figures 3–6 when a C_{4v} model is used.

Furthermore, there is generally very good agreement between the structure parameters determined from the GED data and the

high level B3LYP calculations except for those related to the out-of-plane angles of the isoindole unit which is caused by the low-frequency modes. The B3LYP calculations indicate that replacing the Cl atom with a F atom has neglectable effect on the isoindole structure, replacing the Al atom with a Ga atom has a small but significant effect on the isoindole structure, replacing the peripheral benzene ring with the thiadiazole ring has a small but significant effect on the pyrrole structure, and the structural differences in the pyrrole ring found between FPcAl and FPcGa are very similar to those found between ClPcAl and ClPcGa and between ClTTPzAl and ClTTPzGa.

Acknowledgment. S. Gundersen is acknowledged for workup of the experimental data. T.S. thanks the International Student Quota Program of the University of Oslo for financial support. The Norwegian Research Council (Program for Supercomputing) is acknowledged for computer time.

Supporting Information Available: Calculated (B3LYP/6-311++G**) vibrational frequencies (cm^{-1}) and infrared intensities (km/mol) for ClPcAl, ClPcGa, FPcAl, and FPcGa (Table S1) and for ClTTPzAl and ClTTPzGa (Table S2). Cartesian coordinates from B3LYP/cc-pVTZ calculations for ClPcAl, ClPcGa, FPcAl, FPcGa, ClTTPzAl, and ClTTPzGa, respectively, are given in Tables S3–S8. This material is available free of charge via the Internet at <http://pubs.acs.org>.

References and Notes

- (1) Kadish, K. M.; Smith, K. M.; Guillard, R., Eds. *Application of Phthalocyanines, The Porphyrin Handbook*; Academic Press: San Diego, CA, 2003; Vol. 19.
- (2) Kadish, K. M.; Smith, K. M.; Guillard, R., Eds. *Phthalocyanines: Properties and Materials, The Porphyrin Handbook*; Academic Press: San Diego, CA, 2003; Vol. 17.
- (3) Kadish, K. M.; Smith, K. M.; Guillard, R., Eds. *Phthalocyanines: Spectroscopic and Electrochemical Characterization, The Porphyrin Handbook*; Academic Press: San Diego, CA, 2003; Vol. 16.
- (4) Engel, M. K. *The Porphyrin Handbook, Single-crystal structures of phthalocyanine complexes and related macrocycles*, Academic Press: San Diego, CA, 2003; Vol. 20.
- (5) McKeown, N. B. *Phthalocyanine Materials: Structure, Synthesis and Function*; Cambridge University Press: Cambridge, 1998.
- (6) Leznoff, C. C.; Lever, A. B. P., Eds. *Phthalocyanines - Properties and Applications*; VCH Publishers: New York, Vol1989–1994, Vols. 1–4.
- (7) Samdal, S.; Volden, H. V.; Ferro, V. R.; Garcia de la Vega, J. M.; Gonzalez-Rodriguez, D.; Torres, T. *J. Phys. Chem. A* **2007**, *111*, 4542.
- (8) Strenalyuk, T.; Samdal, S.; Volden, H. V. *J. Phys. Chem. A* **2007**, *111*, 12011.
- (9) Strenalyuk, T.; Samdal, S.; Volden, H. V. *J. Phys. Chem. A* **2008**, *112*, 4853.
- (10) Mihill, A.; Buell, W.; Fink, M. *J. Chem. Phys.* **1993**, *99*, 6416.
- (11) Ruan, C.-y.; Mastryukov, V.; Fink, M. *J. Chem. Phys.* **1999**, *111*, 3035.
- (12) Yamasaki, K.; Okada, O.; Inami, K.; Oka, K.; Kotani, M.; Yamada, H. *J. Phys. Chem. B* **1997**, *101*, 13.
- (13) Wynne, K. J. *Inorg. Chem.* **1984**, *23*, 4658.
- (14) Wynne, K. J. *Inorg. Chem.* **1985**, *24*, 1339.
- (15) Frisch, M. J.; Trucks, G. W.; Schlegel, H. B.; Scuseria, G. E.; Robb, M. A.; Cheeseman, J. R.; Montgomery, J. A., Jr.; Vreven, T.; Kudin, K. N.; Burant, J. C.; Millam, J. M.; Iyengar, S. S.; Tomasi, J.; Barone, V.; Mennucci, B.; Cossi, M.; Scalmani, G.; Rega, N.; Petersson, G. A.; Nakatsuji, H.; Hada, M.; Ehara, M.; Toyota, K.; Fukuda, R.; Hasegawa, J.; Ishida, M.; Nakajima, T.; Honda, Y.; Kitao, O.; Nakai, H.; Klene, M.; Li, X.; Knox, J. E.; Hratchian, H. P.; Cross, J. B.; Bakken, V.; Adamo, C.; Jaramillo, J.; Gomperts, R.; Stratmann, R. E.; Yazyev, O.; Austin, A. J.; Cammi, R.; Pomelli, C.; Ochterski, J. W.; Ayala, P. Y.; Morokuma, K.; Voth, G. A.; Salvador, P.; Dannenberg, J. J.; Zakrzewski, V. G.; Dapprich, S.; Daniels, A. D.; Strain, M. C.; Farkas, O.; Malick, D. K.; Rabuck, A. D.; Raghavachari, K.; Foresman, J. B.; Ortiz, J. V.; Cui, Q.; Baboul, A. G.; Clifford, S.; Cioslowski, J.; Stefanov, B. B.; Liu, G.; Liashenko, A.; Piskorz, P.; Komaromi, I.; Martin, R. L.; Fox, D. J.; Keith, T.; Al-Laham, M. A.; Peng, C. Y.; Nanayakkara, A.; Challacombe, M.; Gill, P. M. W.; Johnson, B.; Chen, W.; Wong, M. W.; Gonzalez, C.; Pople, J. A. *Gaussian 03*, revision B.03; Gaussian, Inc.: Wallingford, CT, 2004.

- (16) Becke, A. D. *J. Chem. Phys.* **1993**, *98*, 5648.
(17) Lee, C.; Yang, W.; Parr, R. G. *Phys. Rev. B* **1988**, *37*, 785.
(18) Krishnan, R.; Binkley, J. S.; Seeger, R.; Pople, J. A. *J. Chem. Phys.* **1980**, *72*, 650.
(19) Frisch, M. J.; Pople, J. A.; Binkley, J. S. *J. Chem. Phys.* **1984**, *80*, 3265.
(20) Dunning, T. H., Jr. *J. Chem. Phys.* **1989**, *90*, 1007.
(21) Porezag, D.; Pederson, M. R. *Phys. Rev. B* **1996**, *54*, 7830.
(22) Halls, M. D.; Schlegel, H. B. *J. Chem. Phys.* **1998**, *109*, 10587.
(23) Johnson, B. G.; Florian, J. *Chem. Phys. Lett.* **1995**, *247*, 120.
(24) Halls, M. D.; Schlegel, H. B. *J. Chem. Phys.* **1999**, *111*, 8819.
(25) Sipachev, V. A. *J. Mol. Struct. (THEOCHEM)* **1985**, *22*, 143.
(26) Sipachev, V. A. *J. Mol. Struct.* **2001**, *67*, 567–568.
(27) Hedberg, L.; Mills, I. M. *J. Mol. Spectrosc.* **1993**, *160*, 117.
(28) Hedberg, L.; Mills, I. M. *J. Mol. Spectrosc.* **2000**, *203*, 82.
(29) Gundersen, G.; Samdal, S.; Seip, H.-M.; Strand, T. G. *Annual Report from the Norwegian Gas Electron Diffraction Group* **1977**, 1980, 1981.
(30) Donzello, M. P.; Agostinetti, R.; Ivanova, S. S.; Fujimori, M.; Suzuki, Y.; Yoshikawa, H.; Shen, J.; Awaga, K.; Ercolani, C.; Kadish, K. M.; Stuzhin, P. A. *Inorg. Chem.* **2005**, *44*, 8539.
(31) Linsky, J. P.; Paul, T. R.; Nohr, R. S.; Kenney, M. E. *Inorg. Chem.* **1980**, *19*, 3131.

JP804105D